

AHP2 is required for bivalent formation and for segregation of homologous chromosomes in *Arabidopsis* meiosis

Carla Schommer[†], Ali Beven, Tom Lawrenson, Peter Shaw and Robert Sablowski*

Department of Cell and Developmental Biology, John Innes Centre, Norwich NR4 7UH, UK

Received 29 April 2003; revised 6 June 2003; accepted 13 June 2003.

*For correspondence (fax +44 1603 450045; e-mail robert.sablowski@bbsrc.ac.uk).

[†]Present address: Department of Molecular Biology, Max Planck Institute for Developmental Biology, Spemannstraße 37-39, D-72076 Tübingen, Germany.

Summary

A new *Arabidopsis* meiotic mutant has been isolated. Homozygous *ahp2-1* (*Arabidopsis* homologue pairing 2) plants were sterile because of failure of both male and female gametophyte development. Fluorescent *in situ* hybridisation showed that in *ahp2-1* male meiocytes, chromosomes did not form bivalents during prophase I and instead seemed to associate indiscriminately. Chromosome fragmentation, chromatin bridges and unbalanced segregation were seen in anaphase I and anaphase II. The *ahp2-1* mutation was caused by a T-DNA insertion in an *Arabidopsis* homologue of *meu13⁺*, which has been implicated in homologous chromosome pairing during meiosis in *Schizosaccharomyces pombe*. Our results suggest that *meu13⁺* function is conserved in higher eukaryotes and support the idea that *Arabidopsis*, yeast and mouse share a pairing pathway that is not present in *Drosophila melanogaster* and *Caenorhabditis elegans*.

Keywords: *Arabidopsis*, meiosis, *meu13⁺*, *HOP2*.

Introduction

Meiosis produces haploid cells from a diploid progenitor through two rounds of cell division. In the first meiotic division, homologous chromosomes are segregated to opposite poles. In the second meiotic division, the two sister chromatids of each chromosome are separated into different cells. During the first division, the homologous chromosomes physically associate and recombine. In most organisms studied, recombination is required for correct segregation of homologues because it holds homologous chromosomes together while they are aligned to the spindle in the first meiotic division (reviewed by Lee and Amon, 2001; Villeneuve and Hillers, 2001).

Most of our understanding of how homologous chromosomes recombine and segregate comes from studies in budding yeast (*Saccharomyces cerevisiae*) and fission yeast (*Schizosaccharomyces pombe*). Before recombination occurs, homologous chromosomes are aligned to each other. This initial pairing is thought to involve unstable contacts between chromosomes (reviewed by Roeder, 1997; Zickler and Kleckner, 1999). In budding yeast, *HOP2* and *MND1* have been proposed to function in the early stages of pairing, monitoring sequence homology to either promote homologue pairing or destabilise pairing between non-homologues (Leu *et al.*, 1998; Tsubouchi and

Roeder, 2002). *meu13⁺* plays a similar role in fission yeast (Nabeshima *et al.*, 2001).

Recombination is initiated by double strand breaks (DSBs) that are catalysed by Spo11p and further processed by Dmc1p, leading to exchange of DNA strands between non-sister, homologous chromatids (reviewed by Keeney, 2001). Absence of recombination in *spo11* mutants disrupts homologue pairing, showing that even if not necessary for the initial stages of pairing, recombination is important to stabilise it (Loidl *et al.*, 1994; Weiner and Kleckner, 1994). In budding yeast, but not in fission yeast, pairing culminates in synapsis when a protein structure called the synaptonemal complex (SC) binds the homologous chromosomes together throughout their length (Zickler and Kleckner, 1999). Genes encoding SC components include *HOP1* (Hollingsworth *et al.*, 1990) and *ZIP1* (Sym *et al.*, 1993). The SC is disassembled before the end of prophase, leaving the homologous chromosomes attached by the crossovers that result from exchange of chromatids during recombination (Zickler and Kleckner, 1999). Both in fission and budding yeast, the two sister chromatids of each homologue are held together by a meiosis-specific cohesin, Rec8p (Klein *et al.*, 1999; Watanabe and Nurse, 1999). To allow resolution of the crossovers and disentanglement of the homologues in anaphase I, Rec8p is removed from the

chromatid arms, but not from the centromeres, ensuring that the sister chromatids remain associated in the first meiotic division (Buonomo *et al.*, 2000).

Less is known about meiosis in multicellular eukaryotes. Homologues of the yeast genes are present and genetic analysis revealed similar functions, e.g. for *SPO11* (Baudat *et al.*, 2000; Grelon *et al.*, 2001; Romanienko and Camerini-Otero, 2000), *HOP1* (Caryl *et al.*, 2000; Zetka *et al.*, 1999) and *REC8* (Bai *et al.*, 1999; Bhatt *et al.*, 1999; Pasierbek *et al.*, 2001). Even when homologous genes are involved, however, the processes in which they participate show variations. For example, in contrast to yeast, mouse and *Arabidopsis*, absence of recombination in *spo11* mutants does not affect synapsis in *Drosophila melanogaster* and *Caenorhabditis elegans* (Dernburg *et al.*, 1998; McKim and Hayashi-Hagihara, 1998). In addition, some genes required for correct chromosome pairing and segregation during meiosis in higher eukaryotes have no yeast homologues, suggesting specialised mechanisms (e.g. *SWI1/DYD* and *SDS* in *Arabidopsis*; Agashe *et al.*, 2002; Azumi *et al.*, 2002; Mercier *et al.*, 2001).

The ability of *D. melanogaster* and *C. elegans* to pair homologues in the absence of recombination suggests that alternative pathways are used for homologue pairing in higher eukaryotes. The use of recombination to stabilise pairing correlates with differences in crossover interference (i.e. the inhibition of crossovers close to each other). Robust crossover interference is seen in *Drosophila*, whereas in yeast and *Arabidopsis*, mathematical models support the idea that two pathways exist for crossover: one which shows interference and another that does not (Copenhaver *et al.*, 2002). In molecular terms, the non-interference pathway seen in yeast and *Arabidopsis* may correspond to the recombination events that are required to stabilise homologue pairing.

The presence of genes homologous to those implicated in the early stages of pairing in yeast, such as *MND1* and *meu13⁺/HOP2*, also correlates with recombination-dependent pairing; homologues of *MND1* and *meu13⁺* are found in *Arabidopsis* and mouse but not in *D. melanogaster* or *C. elegans*. The correlation suggests that these genes carry out conserved functions in the non-interference recombination pathway. Homologues of *MND1* or *meu13⁺* in higher eukaryotes, however, have not been functionally characterised. Here, we describe the effects of a mutation in an *Arabidopsis meu13⁺* homologue.

Results

The ahp2-1 mutant is male and female sterile because of a failure in gametophyte development

The *ahp2-1* (*Arabidopsis* homologue pairing 2) mutant was isolated in a forward screen from a collection of *Arabidopsis*

Landsberg *erecta* lines with T-DNA insertions carrying two selectable markers: kanamycin resistance and constitutive green fluorescent protein (GFP) expression (see the section under Experimental procedures). No abnormalities were seen in *ahp2-1* plants during the vegetative growth phase. Defects became visible in the reproductive phase: the homozygous mutant plants were completely sterile, with short, empty siliques (compare Figure 1a,b). As commonly seen in sterile *Arabidopsis* mutants, *ahp2-1* plants continued to produce flowers while the inflorescence of wild-type siblings had terminated and had begun to senesce. Heterozygous plants were phenotypically indistinguishable from the wild type, showing that the mutant was fully recessive. The progeny of heterozygous plants segregated the mutant phenotype in a 1 : 3 ratio, as expected for a single, Mendelian recessive mutation (19 mutants within a population of 80 plants; $\chi^2 = 0.07$ for 1 : 3 segregation, $\chi^2 = 41.81$ for 1 : 15 segregation).

Cross pollination experiments with wild-type plants showed that *ahp2-1* plants were both male and female sterile. In the cross-pollination experiments, however, the penetrance of the female sterility phenotype was not 100%, and seeds could be obtained with a low frequency (2% that of the wild type after manual pollination).

Closer inspection of the flowers (Figure 1c,f) revealed that the perianth organs were unaffected. The stamens of the mutant flowers, however, were short, with anthers that appeared shrivelled at maturity and released little or no pollen. Irregularly shaped pollen was seen in mutant anthers, but Alexander staining (Alexander, 1987) showed that most of the mutant pollen grains were collapsed and contained no cytoplasm (Figure 1e,h). The pistil of the mutant appeared wild type, but contained abnormal ovules. In most mutant ovules, the gametophyte (embryo sac) appeared only as a very reduced structure (Figure 1d,g) and frequently contained granular material (not shown). While wild-type ovules are anatropous (i.e. asymmetric growth of the integuments orients the micropyle towards the base of the ovule), in mutant ovules, the micropyle was frequently oriented away from the base, suggesting a defect in integument growth.

In summary, the recessive, single locus *ahp2-1* mutation specifically affected reproductive development, with the most severe defects seen in the development of male and female gametophytes.

AHP2 is a homologue of yeast meu13⁺

The *ahp2-1* mutant line had a single locus for kanamycin resistance and GFP expression, which co-segregated with the sterile phenotype, suggesting that the mutation was tagged. Thermal asymmetrically interlaced (TAIL)-PCR revealed that the T-DNA was inserted on chromosome 1 at base 4 568 926, within the fourth exon of predicted gene

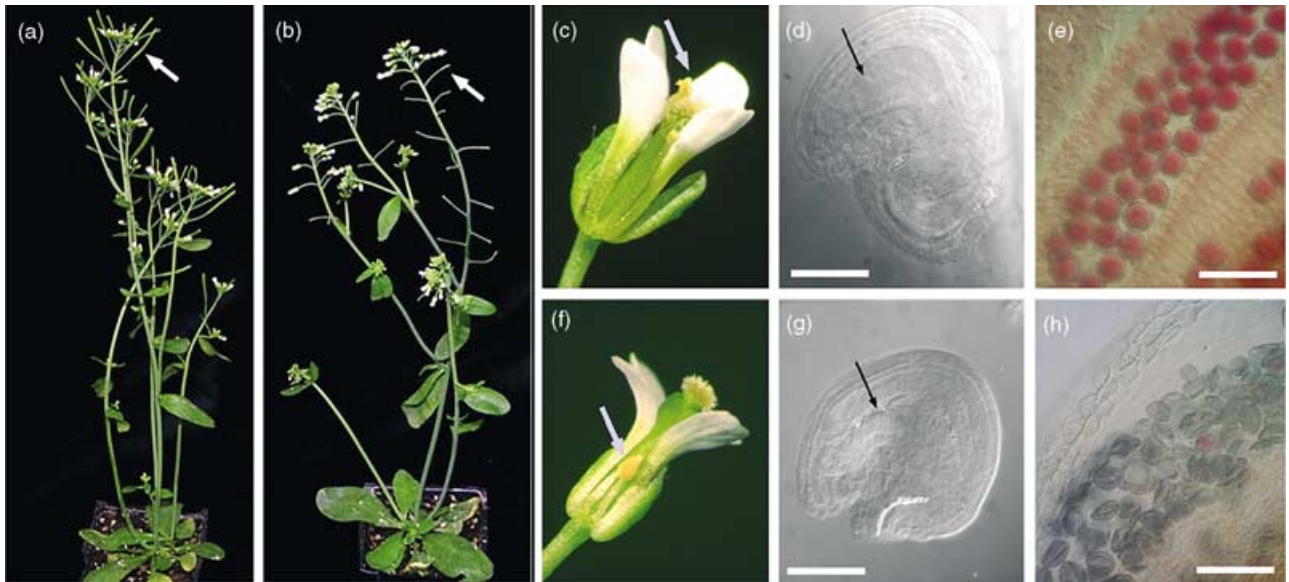


Figure 1. Comparison of wild-type and *ahp2-1* mutant phenotypes.

(a, c–e) Wild type; (b, f–h) *ahp2-1*.

(a, b) Aerial parts of mature plants. The arrow points to a silique in the wild type (a) that fails to elongate in the mutant (b).

(c, f) Close up of mature flowers; the arrows indicate stamens that in the wild type (c) are long and release pollen grains, while in the mutant (f) they remain short with little or no pollen.

(d, g) DIC images of mature ovules; the arrow in (d) points to the large nucleus of the central cell inside the wild-type embryo sac; in (g), the arrow points at a rudimentary or collapsed embryo sac in *ahp2-1*.

(e, h) Viability of pollen inside anthers close to maturity, shown by Alexander staining; the cytoplasm of the viable wild-type pollen stains red (e), while (h) shows collapsed pollen grains in the mutant. The size bars in (d, e, g, h) correspond to 50 μ m.

At1g13330 (The Arabidopsis Information Resource (TAIR) web page: <http://arabidopsis.org/>) (Figure 2a). A Southern blot confirmed the integration in At1g13330 (Figure 2b). Using primers designed to amplify the complete coding sequence, the At1g13330 transcript was detected by reverse transcription (RT)-PCR in wild-type floral buds but not in *ahp2-1* buds, confirming that *ahp2-1* mutants did not accumulate the normal At1g13330 mRNA (not shown). Using primers directed to the region of the transcript upstream of the T-DNA insertion, the levels of At1g13330 transcript were severely reduced in *ahp2-1* compared to those in the wild type, suggesting that the T-DNA insertion disrupted the processing or destabilised the transcript (Figure 2c).

Complementation with the wild-type copy of the gene confirmed that the sterile phenotype was caused by the mutation in At1g13330. Heterozygous plants were transformed with a 4.3-kb genomic fragment containing the wild-type gene, in a vector conferring to gentamycin resistance. The genomic fragment spanned 1.9 kb of sequences upstream of the predicted start codon to 1 kb downstream of the stop codon. We isolated six independent transformant lines that were fully fertile (Figure 2d,e) in spite of being homozygous for the T-DNA insertion in At1g13330, based on kanamycin resistance and GFP expression. Fertility in these lines co-segregated with gentamycin

resistance, confirming that it depended on the transgene. Six additional lines were partially complemented. In these plants, the first three to four flowers were sterile before flowers developed into normal siliques containing fertile seeds; at later stages, the plants occasionally had sterile flowers (not shown). Together, the results showed that At1g13330 is *AHP2*.

AHP2 cDNA was cloned by RT-PCR from floral tissue (Columbia ecotype), using primers designed according to the predicted start and stop codons for At1g13330. The 681-bp-long cDNA confirmed the predicted intron/exon structure and coded for a 226-amino-acid peptide (Figure 3). BLASTP searches (Altschul *et al.*, 1997) database identified no related proteins encoded in the *Arabidopsis* genome, in agreement with the Southern blot data shown in Figure 2(b) (the BLAST alignments can be seen on the MatDB web page: <http://mips.gsf.de/proj/thal/db/index.html>). In other plants, homology to uncharacterised genes in maize and rice was found (not shown). Outside plants, homologues were identified in mammals and yeast (Figure 3). All proteins were similar in size (203–226 amino acids) and shared homology throughout their sequence. The closest *AHP2* homologue outside the plant kingdom is the mouse TBPIP, with 48% similarity (BLAST expect value $5e^{-25}$). Mammalian Tat-binding protein 1-interacting proteins (TBPIPs) have been cloned based on their interaction

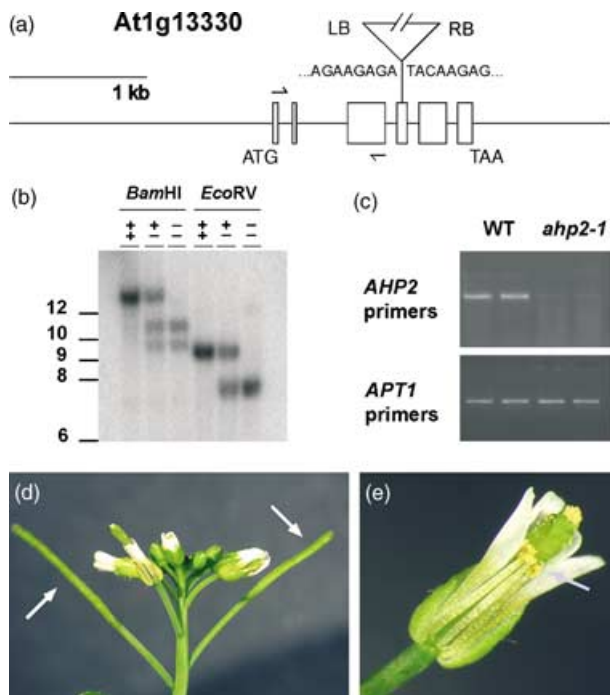


Figure 2. Molecular identification of *AHP2*.

(a) Location of the T-DNA insertion of *ahp2-1* mutant, determined by TAIL-PCR. The At1g13330 gene is described in the TAIR database (<http://arabidopsis.org/>). Open boxes represent exons; start and stop codons are indicated below the diagram. The inverted triangle represents the T-DNA insert (not to scale); LB and RB indicate left and right borders, respectively. The nucleotide sequence interrupted by the T-DNA within exon 4 is also shown. The arrows above exons 1 and 6 indicate the position of the primers used to clone the *AHP2* cDNA. These primers were also used in the RT-PCR shown in (c) and to amplify the genomic fragment used to probe the Southern blot in (b). (b) Southern blot of genomic DNA from wild-type (Landsberg *erecta*) plants (marked +/+), heterozygous (+/-) and homozygous *ahp2-1* plants (-/-), digested with *Bam*HI and *Eco*RV and probed with *AHP2*. The single *Bam*HI and *Eco*RV *AHP2* fragments seen in the wild-type are shifted in the mutant because of the presence of additional *Bam*HI and *Eco*RV sites in the T-DNA. The heterozygous plants showed the expected superimposition of the wild-type and mutant restriction patterns. The numbers on the left indicate molecular size in kilobases.

(c) Detection of *AHP2* transcripts or *APT1* transcripts (control) by RT-PCR in RNA extracted in duplicate from the wild type and from *ahp2-1* inflorescences. The position of the primers used for *AHP2* amplification are indicated in (a).

(d, e) Complementation of the *ahp2-1* mutant with the 4.3-kb genomic fragment containing At1g13330. One representative complemented line is shown (homozygous for *ahp2-1* based on the segregation of the GFP and kanamycin markers present in the T-DNA), with full restoration of fertility. Arrows show elongated siliques in (d) and production of pollen grains in (e). In the flower shown in (e), fertilisation has already occurred and the pistil has started to elongate.

with TBP, which is a part of the 26S proteasome. Based on the expression of the mouse and human TBPIPs in testes, a role in male meiosis has been speculated (Ijichi *et al.*, 2000; Tanaka *et al.*, 1997). *AHP2* was also significantly similar to *Meu13p* from *S. pombe* (BLAST expect value $6e^{-16}$). Similarity between *AHP2* and *HOP2* was more limited, consistent with the fact that *S. cerevisiae* is a more distant relative of higher eukaryotes than *S. pombe* is. Nevertheless, the

fact that *AHP2* was highly similar to all homologues of *HOP2* in other organisms clearly places *AHP2* and *HOP2* in the same protein family.

Both *meu13⁺* and *HOP2* have been implicated in homologue pairing during meiosis (Leu *et al.*, 1998; Nabeshima *et al.*, 2001). Thus, the published data on the *AHP2* homologues suggested that the failure in gametophyte development in the *ahp2-1* mutant could be caused by a defect in meiosis.

ahp2-1 meicytes have entangled chromosomes and fail to form bivalents

To investigate whether the *ahp2-1* mutant had a defect in meiosis, we compared meicytes in *ahp2-1* and in the wild type. We focused on male meicytes, which could be analysed by fluorescent *in situ* hybridisation (FISH) in sufficiently high numbers. Chromosome morphology was examined in male meicytes by staining with 4',6-diamidino-2-phenylindole (DAPI). Formation of bivalents during prophase I was monitored by FISH with a probe directed to the nucleolar organising regions (NORs). *Arabidopsis* has five chromosomes, two of which (numbers 2 and 4) have NORs near their telomeres (Armstrong and Jones, 2003).

The results shown here focus on the mid-prophase to telophase of the first meiotic division, when differences between *ahp2-1* and the wild type were first seen. Figure 4(a) shows wild-type meicytes at the pachytene stage of prophase I, when synapsed chromosomes were visible and all NORs were clustered. This initial association of NORs matched the transient clustering of telomeres that was also seen in pachytene (Armstrong and Jones, 2003). By the beginning of metaphase I, five sets of paired chromosomes were clearly seen with NOR signals marking the bivalents (paired set of homologous chromosomes) 2 and 4 (Figure 4b). In anaphase, the homologues were separated giving two sets of five univalents (Figure 4c,d) and initially four FISH signals, then eight, when sister chromatids were partially separated (Figure 4d). Separation of the two sets of five chromosomes, each set with two pairs of matched NOR signals, was complete in telophase (Figure 4e).

In *ahp2-1* meicytes, clustering of the NORs occurred normally in mid-prophase (Figure 4f), although the chromosome strands were not as clearly visible as in the wild-type pachytene stage. Subsequent prophase stages such as diplotene and diakinesis could not be clearly defined in the mutant. By metaphase I, the chromosomes looked entangled (Figure 4g). A variable number of discrete chromosomes were visible, but the total number of separate chromosomes was consistently less than 10, indicating that at least some of the chromosomes were connected to each other. Within the tangle of chromosomes, however, four clearly separate NORs were detected, showing that homologues were not associated (Figure 4g). In anaphase, two

Figure 3. Alignment between the AHP2 protein and non-plant homologues.

Black and grey boxes indicate highly conserved and partially conserved amino acids, respectively. The accession numbers are: AAG09555.1 for *A. thaliana* AHP2; BAA23155.1 for *Mus musculus* TBPIP; BAA92872.1 for *Homo sapiens* TBPIP; BAB17055.1 for *S. pombe* Meu13p; AAC31823.1 for *S. cerevisiae* HOP2p.

AHP2	1	MAP-KSDN-----TEA--IIVLNFEVNEQNKPLNTQVAADALQKFN-LKKTAVQKALDS
Hs	1	MS--KCRALAAAGAAAG-----ILLRYLQEQNRPYSSQDVDFGNLQREHGLGKAVVVKTLLEQ
Mm	1	MS--KSRALAAAGAPG-----ILLRYLQEQNRPYSAQDVDFGNLQKEHGLGKAAVVKALDQ
Sp	1	MA--KAKEVKAKPIKGEFAEKLVYEYLKRTNRPYSATDVSANLK--NVVSKQVAQKALEQ
Sc	1	MAPKKKSNDRAIQAKCSFAEQLEEDYLVSYKPPSVNDIVQNLH--NKVTKTTATKALEN
AHP2		LADAGKITPKEYGKOKIYIARQDQFEINPSEELAQMK-EDNAKIQEQIQEKKKTIISDVES
Hs		LAQOGKIKBKMYGKOKIYFADQDFDMVSDADLQVLDGK-IVALTAKVQSLQOSCRVMEEA
Mm		LAQGGKIKBKTYGKOKIYFADQDFDMVSDADLHGLDAS-IVALTAKVQSLQOSCRVMEEA
Sp		LRDTGLIIEGKLYGKQSVFVCLQDPLAAAPPEELAEEMKQ-IQELKDEVSVVKITLYKEKCI
Sc		LVNEKRIIVSKTFAKIIITYSCNEQDTALPSNIDPSQFDFETVQLRNDIIELEERDKSTAKD
AHP2		EIKSLQSNLTLEELQEKDAKLRKEVKEMEELVKLRECIIT-LVRPEDKKAVEDMYADKIN
Hs		ELKELSSALTTPEMQKETQELKKECAGYRERLKNIK-AATNHVTPEEKEQVYRERQKYCK
Mm		ELKELSSALTTPEMQKETQELKKECAQYTERLKNIK-AATNHVTPEEKEQVYRDRQKYCK
Sp		ELQALNNSLSPAEIREKIQSIDKEIEETSSKLESLRNQTVKQLSKEAMQKTDKNY-DFAK
Sc		ALDSVTKPEPENEDLTIIEENEELKKIESKLSLQ-DWDPANDEIVKRIIMSEDTLLQK
AHP2		QWRKRKRFRDIWDITVTENS--PKDVKLKEELGIEYDEDVGLSFQAYADLIQHKKRPR
Hs		EWRKRKRMTTELSPALLEGY--PKSKKOFFEEVGIETDEDYNTLPPD 218
Mm		EWRKRKRMTTELCPALLEGY--PKSKKOFFEEVGIETDEDHNTLPPD 218
Sp		KFSNRKRMFYDLWHLITDSLENPK--QLWEKLGFEETGPIIDN 217
Sc		EITKRSKICCKPN-----CYNKGLSVPEKYE 204
AHP2	GQ	226

masses of chromatin were pulled to opposite poles but the chromosomes were not clearly distinguished (Figure 4h). Chromatin bridges frequently linked both chromatin masses and what appeared to be chromosome fragments remained at the metaphase plate (Figure 4h,i). Unequal numbers of NORs were pulled to each pole; NOR signals sometimes coincided with the chromatin bridges (Figure 4h,i) and with the fragments left behind at the centre of the cell (Figure 4j). Between telophase and the end of prophase II (Figure 4i,j), condensed chromosomes or chromosome fragments became visible in variable numbers but less than 10. The NOR signals were variable (between 4 and 10) and unevenly distributed between the two poles of the cell (Figure 4i,j). The defects in the second meiotic division paralleled those described above, with formation of chromatin bridges during anaphase II and uneven distribution of NORs (not shown).

The results described above showed that *ahp2-1* plants were defective in forming bivalents and in chromosome segregation during meiosis. It seems likely that the subsequent defects in gametophyte development and fertility in *ahp2-1* mutants are because of the uneven chromatid distribution during meiosis and consequent genetic imbalance of the meiotic products.

AHP2 is expressed in both reproductive and vegetative tissues and is localised in the nucleus

meu13⁺ is expressed specifically during meiosis. To verify if the same is true for *AHP2*, we monitored its expression in vegetative tissues (seedlings, leaves), in floral tissue at early and late stages of development and in mutant flowers that do not develop reproductive organs and therefore lack meiocytes (*agamous* mutant; Bowman *et al.*, 1989).

Northern blots and *in situ* hybridisation failed to detect *AHP2* mRNA, presumably because of low expression. Semi-quantitative RT-PCR detected comparable expression in reproductive and vegetative tissues (Figure 5). In flowers, expression was not associated exclusively with reproductive organs, as *AHP2* was clearly expressed in *agamous-3* buds. A reporter line with the *uidA* reporter controlled by sequences upstream of the *AHP2* coding sequence showed widespread expression (not shown), supporting the idea that *AHP2* is expressed in both vegetative and reproductive tissues.

We also attempted to monitor expression and localisation of the AHP2 protein in transgenic plants containing GFP or GUS fused in frame to the C-terminus of the AHP2 coding sequence, within the genomic fragment that had been used to complement the *ahp2-1* mutant. No lines were obtained that expressed either fusion proteins, suggesting that the fusion product might be deleterious to plant growth. To circumvent the possibility of deleterious effects of the GFP fusion protein on cell division or development, localisation of a GFP-AHP2 fusion was monitored in a transient assay by bombardment of a *35S:GFP-AHP2* construct into onion epidermal cells. Figure 6(a) shows that GFP-AHP2 was localised in the nucleus in contrast to GFP alone (Figure 6c), indicating that AHP2 carries nuclear localisation signals and that the protein can accumulate in vegetative tissues.

Discussion

Several mutants have been described in which homologous chromosomes fail to associate, forming univalents that segregate randomly in anaphase I. Most of these mutations prevent chromosome synapsis by either disrupting

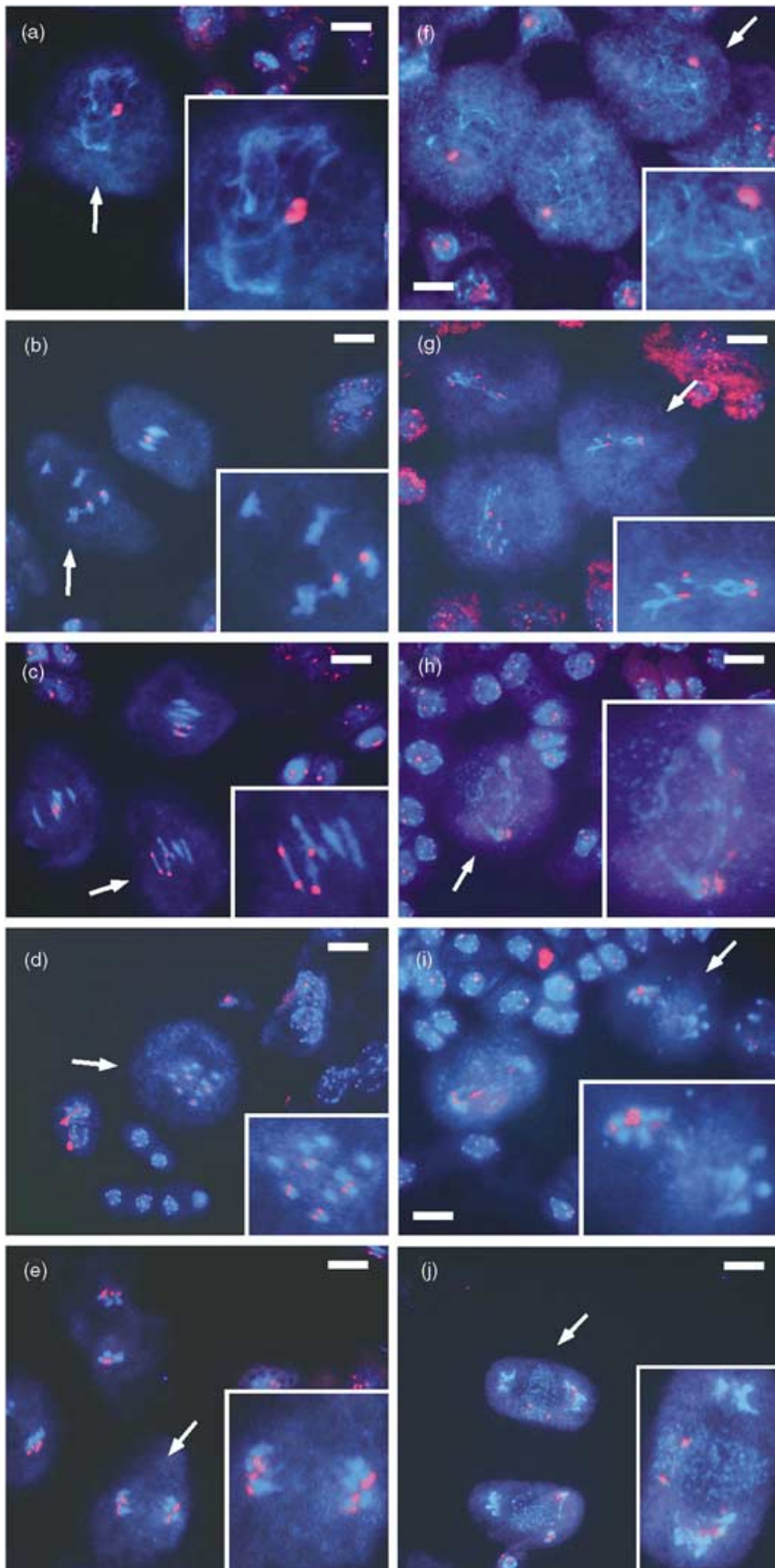


Figure 4. Chromosome pairing and segregation in male meiocytes of wild-type and *ahp2-1* mutant plants.

The pictures are superimposed images of DAPI fluorescence (blue, showing condensed chromatin) and FISH (red) with a probe for NORs. (a–e) Wild-type meiocytes; (f–j) *ahp2-1* meiocytes. The arrows point at cells that are shown at higher magnification in the insets. The size bars (for the lower magnification, not for the insets) correspond to 10 μ m.

(a) Wild-type meiocyte at pachytene stage. The NORs are clustered.

(b) Early metaphase I (cell marked with arrow) and early anaphase (upper cell) in wild-type meiocytes. Note the single NOR signals on two of the five bivalents seen in metaphase.

(c) Anaphase I in wild-type meiocytes. Note the four NOR signals seen when the homologous chromosomes are segregated to opposite poles of the cell.

(d) Late anaphase I in the wild type, showing segregation of the two groups of five univalents. In each group, two univalents have NORs (corresponding to chromosomes 2 and 4). Note that each univalent has two adjacent NOR signals, visible after the partial separation of sister chromatids.

(e) Telophase I in the wild type. Note the two groups of five univalents, each with four NOR signals.

(f) *ahp2-1* meiocytes at a stage comparable to that shown in (a). The NORs are clustered.

(g) Metaphase I in *ahp2-1* meiocytes. Each cell has four NOR signals (contrast with the two signals seen in b). The number of chromatids is difficult to determine because the chromosomes appear entangled.

(h) Anaphase I in the *ahp2-1* mutant. Note the two masses of chromatin pulled to opposite poles of the cell, with chromatin bridges and fragments in between.

(i) Telophase I in *ahp2-1* meiocytes (arrow). Note the uneven segregation of NORs. The second meiocyte on the left side is in late anaphase; NOR signals coincide with chromatin bridges between the two poles of the cell.

(j) Late prophase II (arrow) and anaphase II (cell at the bottom) in *ahp2-1*. Note the uneven segregation of NORs and the NOR signals on chromatin fragments that remained in the metaphase plate.

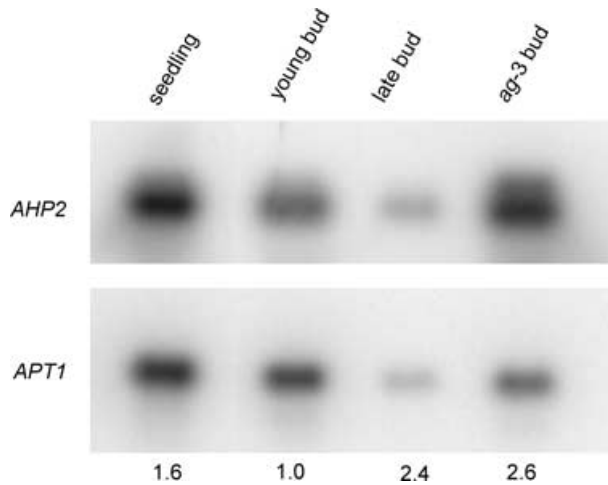


Figure 5. Detection of *AHP2* transcripts in seedlings and flowers. RT-PCR was performed with RNA from wild-type seedlings, young or late floral buds, and buds from the *ag-3* mutant, with primers that amplified *AHP2* or *APT1* (control; Moffatt *et al.*, 1994) cDNAs. The number of PCR cycles was chosen to give visible signals after Southern blotting of the PCR products, before the amplification reached plateau. The numbers below the Southern blots indicate the relative *AHP2* levels detected in each sample, with the signal in each tissue divided by the *APT1* signal and with the value for young buds set to 1.0.

recombination or interfering with the SC, as seen in *spo11*, *dmc1*, *hop1* in yeast and in their *Arabidopsis* counterparts (Bishop *et al.*, 1992; Caryl *et al.*, 2000; Couteau *et al.*, 1999; Grelon *et al.*, 2001; Hollingsworth *et al.*, 1990; Klapholz *et al.*, 1985; Shinohara *et al.*, 1992). The yeast *hop2* mutant, however, is unique in that defective homologue pairing is combined with synapsis between non-homologous

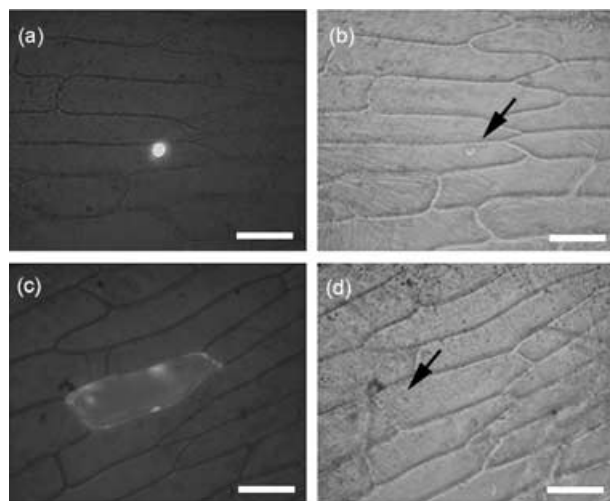


Figure 6. Nuclear localisation of GFP-AHP2 during transient expression in onion epidermal cells. The arrow indicates the nucleus. The size bar corresponds to 100 μm . (a, b) Cell transformed with *35S::GFP-AHP2*; in (a), GFP fluorescence; in (b), bright field image. (c, d) Cell transformed with *35S::GFP* control; in (c), GFP fluorescence; in (d), bright field image.

chromosomes, resulting in a mass of indiscriminately associated chromosomes (Leu *et al.*, 1998). Deletion of *meu13*⁺, the *HOP2* homologue in *S. pombe*, also caused a defect in homologue pairing that is not followed by indiscriminate synapsis because *S. pombe* is asynaptic (Nabeshima *et al.*, 2001). Although we have not been able to directly monitor the early stages of chromosome pairing in *Arabidopsis*, the phenotype seen in *ahp2-1* meiocytes is reminiscent of that reported for *hop2* mutants. At the end of prophase I, homologous chromosomes were not associated with each other, but instead of remaining as univalents, had formed a mass of entangled chromosomes. Together with the fact that *AHP2* is the only homologue of *meu13*⁺ identifiable in the *Arabidopsis* genome, our data suggest that *meu13*⁺/*HOP2* function is conserved in *Arabidopsis*.

In addition to having a defect in homologue pairing, the Δ *meu13* and *hop2* mutants accumulate unrepaired DSBs (Leu *et al.*, 1998; Nabeshima *et al.*, 2001). In the *hop2* mutant, the accumulated DSBs cause arrest of meiosis at the pachytene stage. This recombination checkpoint is also present in animals, where it triggers apoptosis instead of arrest (reviewed by Roeder and Bailis, 2000). In *Arabidopsis*, the pachytene checkpoint seems to be absent or less stringent because meiosis is completed in *dmc1* mutants (Couteau *et al.*, 1999). This view is consistent with the fact that, unlike in yeast *hop2* mutants, meiosis was not arrested in the *ahp2-1* mutant.

The absence of a checkpoint arrest in *ahp2-1* mutants allowed us to monitor chromosome behaviour beyond the pachytene stage. One of the features of *ahp2-1* meiocytes was that chromosomes not only became entangled during prophase but also remained attached during anaphase and formed chromatin bridges. If pairing between non-homologous chromosomes or non-homologous parts of chromosomes occurs in *ahp2-1*, as it does in *hop2*, one explanation for these bridges could be aberrant crossover and exchange of DNA strands between non-homologous chromosomes or parts of chromosomes. Alternatively, the chromosome entanglement during anaphase could be the consequence of a failure to dissolve ectopic SC formed during prophase I. This would mirror the proposed role of HOP2 in promoting homologue pairing by destabilising ectopic synapses (Leu *et al.*, 1998).

In addition to chromatin bridges, *ahp2-1* meiocytes showed chromosome fragmentation in anaphase I. Breakage could be a consequence of tension when attached chromosomes are pulled to opposite ends. However, chromosome fragments appeared to remain in the centre of the cell at the beginning of anaphase, suggesting that fragmentation preceded pulling of the chromosomes. This could result from unresolved DSBs. If, like Δ *meu13* and *hop2* mutants, *ahp2-1* meiocytes accumulate unrepaired DSBs, the chromatids should initially remain attached by cohesin in spite of forming the DNA breaks. When sister chromatid

cohesion is partially dissolved in anaphase I, the broken chromatids could drift as chromosome fragments.

Of the *Arabidopsis* meiotic mutants described so far, *syn1* (also known as *dif1*) has the phenotype most similar to that of *ahp2-1* (Bai *et al.*, 1999; Bhatt *et al.*, 1999). In *syn1* meiocytes, prophase stages beyond early leptotene are abnormal, with entangled chromosomes, although in this case, homologue association has not been monitored by FISH. As in *ahp2-1*, *syn1* meiocytes showed entangled chromatin masses, chromosome fragmentation and chromatin bridges in metaphase and anaphase I. *SYN1/DIF1* encodes an *Arabidopsis* homologue of the meiotic cohesin REC8 (Bai *et al.*, 1999; Bhatt *et al.*, 1999). In addition to a role in sister chromatid cohesion, REC8 homologues have been implicated in recombination in both meiosis and mitosis (Klein *et al.*, 1999). The chromosome entanglement and chromatin bridges in *syn1* mutants are not readily explained as a direct consequence of a failure to maintain sister chromatid cohesion, leading to the suggestion that these defects are because of aberrant recombination events (Bai *et al.*, 1999; Bhatt *et al.*, 1999). The very similar meiotic phenotypes in *syn1* and *ahp2-1* suggest that both genes could work in the same process, implying a role for *AHP2* in meiotic recombination. A role in the initial stages of recombination is also consistent with the accumulation of DSBs in the $\Delta me13$ and *hop2* mutants.

One difference between *AHP2* and *HOP2/meu13⁺* (and an additional similarity to *SYN1*) is that *AHP2* mRNA does not accumulate exclusively during meiosis. Expression in vegetative tissues was also seen for other *Arabidopsis* genes for which mutants suggested meiosis-specific functions as seen in *SYN1/DIF1*, *ASY1* and *MS5* (Bai *et al.*, 1999; Bhatt *et al.*, 1999; Caryl *et al.*, 2000; Glover *et al.*, 1998). It is also noteworthy that the mammalian *HOP2* homologues are expressed in tissues where meiosis is absent (Ijichi *et al.*, 2000; Tanaka *et al.*, 1997). *ahp2-1* is fully recessive and is likely to be a severe or null allele, because the T-DNA insertion caused a drastic reduction in transcript levels, and even if some mutant mRNA were translated, it would produce a truncated protein with the C-terminal half missing. Given that *AHP2* is a single-copy gene in *Arabidopsis*, it is unlikely that any vegetative functions of *AHP2* under normal growth conditions would be covered by gene redundancy. It remains to be tested, however, whether *ahp2-1* mutants are sensitive to DNA damage, which would suggest a role in recombination-dependent DNA repair.

The exact molecular function of the *AHP2* protein or any of its homologues remains an open question. It is intriguing that the mouse and human homologues (TBIIP:TBP-1-interacting protein) interacted in the yeast two-hybrid assay with TBP-1, which is a subunit of the 26S proteasome (Ijichi *et al.*, 2000; Tanaka *et al.*, 1997). Interaction with the proteasome suggests a role in targeted proteolysis, which could be part of the mechanism by which *HOP2* and

homologues (including *AHP2*) could destabilise ectopic chromosome pairing. However, our own yeast two-hybrid experiments (Schommer and Sablowski, unpublished) failed to detect an interaction between *AHP2* and RPT5a, which is the closest *Arabidopsis* homologue of TBP-1 (Fu *et al.*, 2001). A direct role in targeted proteolysis is also not readily compatible with the report that the human and rat homologues function as transcriptional co-activators that bind to nuclear receptors (Ko *et al.*, 2002).

Whatever the exact molecular function of *AHP2* and its homologues is, the fact that the *ahp2-1* mutant had meiotic defects that are consistent with a function similar to that of *meu13⁺/HOP2*, together with the presence of homologous genes in mouse and human, suggest that *meu13⁺/HOP2* function is widely conserved. The absence of homologues in *D. melanogaster* and *C. elegans* adds to a list of exceptional features of meiosis in these species, including the absence of *DMC1* homologues and the *SPO11*-independent chromosome synapsis. The co-ordinated absence of *meu13⁺*, *DMC1* and of *SPO11*-dependent synapsis in *D. melanogaster* and *C. elegans* may reflect the presence of an alternative pathway to promote homologue pairing in these organisms (Villeneuve and Hillers, 2001). The fact that the homologues of *meu13⁺* and *DMC1* and *SPO11*-dependent synapsis are co-ordinately expendable suggests that they function together in a conserved pathway.

Experimental procedures

Molecular biology methods

Standard molecular biology techniques were used for Southern blotting and for plasmid construction (Sambrook *et al.*, 1989). The plasmid used to generate the T-DNA insertional mutant was derived from pCGN18 (Krizek and Meyerowitz, 1996) with the mGFP5-ER cDNA (Haseloff, 1999) being cloned as a *Bam*HI-*Xba*I insert between the 35S promoter and the NOS terminator. The plasmid containing the *AHP2* gene for complementation was derived from pZP222 (Hajdukiewicz *et al.*, 1994), containing the *AHP2* genomic sequence (bp 44221–48561 on BAC T6J4) removed as an *Eco*RV/*Sal*I fragment from the cosmid 87H23 (JatC library, made by Ian Bancroft; see: <http://www.jic.bbsrc.ac.uk/staff/ian-bancroft/resources.htm>). To generate the *AHP2*-GFP and *AHP2*-GUS fusions, the GFP (from pAVA121; von Arnim *et al.*, 1998) or GUS coding sequences (from pRAJ275; Jefferson, 1988) were inserted within the *AHP2* genomic fragment described above (using a *Xho*I site), in frame with amino acid 223 of the *AHP2* coding sequence. The correct fusions were confirmed by sequencing with ABI Big Dye kit and an ABI 3700. To clone the *AHP2* cDNA, RNA was extracted from inflorescences of *Arabidopsis* (Columbia ecotype), using TRIZOL (Sigma-Aldrich Co. Ltd., Poole, UK), following the manufacturer's instructions. DNase I-treated total RNA was reverse-transcribed using moloney murine leukemia virus (MMLV) reverse transcriptase (Stratagene Ltd., Cambridge, UK). The *AHP2* coding sequence was PCR-amplified using *Pwo* polymerase (Roche Diagnostics Ltd., Lewes, UK), primers *AHP2F* (5'-TTTCGGGATCCATGGCTCCTAAATCGGATAACACCGA-3') and *AHP2R* (5'-AACTTATCTAGAAATTACTGTCCTCGAGGCCTCTTT-

TACC-3') and 35 cycles of 94°C/30 sec, 52°C/1 min, 72°C/2 min. The product was cut with *Bam*HI and *Xba*I and cloned into pBluescript KS(-) (Stratagene) cut with the same enzymes, and the cDNA sequence was confirmed using the ABI Big Dye kit and an ABI 3700. The 35S:*GFP-AHP2* construct for bombardment into onion cells was derived from pAVA121 (von Arnim *et al.*, 1998), which was opened with *Bgl*II/*Xba*I and ligated to the AHP2 cDNA to generate an in frame fusion with GFP. The 35S:*GFP* control was pAVA121.

TAIL-PCR was carried out as described by Liu and Whittier (1995). To analyse expression by RT-PCR, RNA was extracted with Trizol from seedlings or floral buds and reverse-transcribed as described above. Amplification was with Taq polymerase (Roche) in the standard buffer recommended by the manufacturer.

To check *AHP2* expression in wild-type and mutant buds (Figure 2c), RT was primed with oligonucleotide AHP2B (see below) and PCR amplification was with primers AHP2C (5'-TGATTCTGATTCCACATCACTG-3') and AHP2D (5'-AAATCGGATAACACCGAAGC-3'). The constitutive control was *APT1* (Moffatt *et al.*, 1994), amplified with primers APT1 (5'-CCTTCCCTTAA-GCTCTG-3') and APT2 (5'-TCCCAGAATCGCTAAGATTGCC-3'). For quantitative comparison in different tissues (Figure 5), the primers used for *AHP2* were AHP2A (5'-GGTGAGGCCAGAAGACAAA-3') and AHP2B (5'-CCTCGAGGCCTTTTTACC-3'). The PCR products were detected by Southern blotting, exposed to a Phosphor-Imager screen (Amersham Biosciences UK Ltd., Little Chalfont, UK) and quantified using the IMAGEQUANT software (Molecular Dynamix). A range of PCR cycles (20–40) was tried for both *AHP2* and *APT1* to choose conditions where amplification had not reached plateau. These conditions were: 94°C/30 sec, 53°C/60 sec, 72°C/90 sec; 30 cycles for *AHP2*; and 20 cycles for *APT1*.

Plant transformation and growth

Arabidopsis Landsberg erecta seeds were stratified on wet filter paper at 4°C for 4 days before germinated on soil and grown in a greenhouse at approximately 21°C with 16-h light (daylight supplemented with artificial lights in the evening)/8-h dark cycles. For crossing, four to five flowers of pollen-acceptor plants were emasculated approximately 2 days before pollination. The remaining flowers and buds of an inflorescence and the inflorescence meristems were removed. Mature stamens were removed from pollen donor plants with tweezers, and pollen was dabbed on pistils of pollen-acceptor plants.

Arabidopsis was transformed by the floral dip method (Clough and Bent, 1998). *Agrobacterium* strains were ASE for pCGN18 derivatives and GV3101 for pZP222 derivatives. Transformants were selected on GM medium (Valvekens *et al.*, 1988) with 50 µg ml⁻¹ kanamycin (for pCGN derivatives) or 100 µg ml⁻¹ gentamycin (for pZP222 derivatives). For growth on plates, seeds were surface-sterilised for 5 min in 50% v/v commercial bleach with 0.1% Tween-20, then plated on GM medium. After stratification at 4°C for 4 days, the seedlings grew at 18–20°C with 16-h light (fluorescent lights at approximately 100 µmol photons m⁻² sec⁻¹) and 8-h dark cycles. Transformants were moved to soil after 1–2 weeks.

Transient transformation assays in onion epidermal cells were as described by Varagona *et al.* (1992), except that 10 µg of plasmid DNA (prepared with the Qiagen kit) was precipitated onto 2 mg of 1.6 µM gold particles. The bombardment was carried out with the Biolistic Particle Delivery System, Model PDS-1000 (DuPont Inc., Wilmington, DE, USA), at a setting of 12 kV. The plates containing the onion cells were incubated at 30°C covered in cling film to avoid drying out of the cells for 6 h, before examination under a fluorescence microscope with FITC filter settings.

Microscopy

Staining for pollen viability was carried out, as published by Alexander (1987), with the following changes: inflorescences were fixed for 1–3 h in FPA50 (5 ml formaldehyde 37%, 5 ml propionic acid, 90 ml ethanol), anthers were dissected on a slide, Alexander stain was prepared without phenol, 2 ml glacial acetic acid was used per 100 ml stain and the minimal time for staining was 20 min. Differential interference contrast (DIC) imaging of cleared ovules was performed as described by Boissard-Lorig *et al.* (2001).

Fluorescent *in situ* hybridisation was adapted as described by Schwarzmacher (2000). Inflorescences were collected shortly after bolting and fixed in 3 : 1 ethanol:acetic acid at 4°C for at least 1 week. The fixed buds were washed two times for 5 min in citrate buffer (0.01 M trisodium citrate, 0.01 M citric acid; pH 4.5), hydrolysed in 0.2 M HCl for 10 min at 37°C, washed again in citrate buffer for 5 min and incubated in 2% cytohelicase (Sigma) in citrate buffer for 10 min at room temperature. After two more washes in citrate buffer, 0.8-mm-long buds were selected and dissected in 45% acetic acid. Isolated anthers were squashed under a cover-slip, frozen in liquid nitrogen, the cover-slip was flicked off and the slide was air-dried. The slides were washed two times for 5 min in 2× SSC (20× SSC: 3 M sodium chloride, 300 mM trisodium citrate; pH 7) and fixed for 15 min at room temperature in 4% (w/v) formaldehyde, freshly prepared from paraformaldehyde in PEM buffer (50 mM PIPES/KOH, pH 6.9; 5 mM EGTA; 5 mM MgSO₄). After two more washes in 2× SSC, the slides were dehydrated through an ethanol series (70, 90 and 100%, 5 min each) and air-dried. Each slide was hybridised to 200 ng of the NOR probe, prepared from BAC F28F7, labelled by nick translation with biotin-16-dUTP (Roche Diagnostics Ltd.). The probe was diluted in hybridisation mix (50% de-ionised formamide, 20% dextran sulphate, 0.1% sodium dodecyl sulphate, 10% 20× SSC and 1 µg of sonicated salmon sperm as blocking DNA), denatured at 95°C for 5 min and cooled on ice for 5 min. The probe applied to each slide was covered with a plastic cover-slip to limit evaporation, and hybridisation was performed in an Omnislide thermal-cycler (Thermo Electron Corporation, Needham Heights, MA, USA) with initial target denaturation at 78°C and subsequent hybridisation at 37°C overnight. The slides were washed two times for 5 min in each of the following: 2× SSC at 42°C, 20% formamide/0.1× SSC at 42°C, 2× SSC at 42°C, 2× SSC at room temperature and 4× SSC/0.2% Tween at room temperature. The slides were then incubated at room temperature for 1.5 h with extravidin CY3 (Sigma) diluted 1 : 200 in 3% BSA (Sigma) in 4× SSC/0.2% Tween-20. After three 10 min washes in 4× SSC/0.2% Tween-20, the slides were incubated in DAPI (1 µg ml⁻¹ H₂O; Sigma) for 30 min, washed three times in water for 10 min, mounted in vectashield (Vector Laboratories Ltd., Peterborough, UK) and viewed on a Nikon Eclipse 600 microscope. The images from the CY3 and DAPI channels were superimposed using ADOBE PHOTOSHOP 5.0.

Acknowledgements

We are grateful to Anuj Bhatt for critical reading of the manuscript. C.S. received a John Innes Centre Foundation Studentship. Work in the R.S. lab is funded by BBSRC and the European Union-FPV.

References

- Agashe, B., Prasad, C.K. and Siddiqi, I. (2002) Identification and analysis of DYAD: a gene required for meiotic chromosome organisation and female meiotic progression in *Arabidopsis*. *Development*, **129**, 3935–3943.

- Alexander, M.P. (1987) A method for staining pollen tubes in pistil. *Stain Technol.* **62**, 107–112.
- Altschul, S.F., Madden, T.L., Schaffer, A.A., Zhang, J., Zhang, Z., Miller, W. and Lipman, D.J. (1997) Gapped BLAST and PSI-BLAST: a new generation of protein database search programs. *Nucl. Acids Res.* **25**, 3389–3402.
- Armstrong, S.J. and Jones, G.H. (2003) Meiotic cytology and chromosome behaviour in wild-type *Arabidopsis thaliana*. *J. Exp. Bot.* **54**, 1–10.
- von Arnim, A.G., Deng, X.W. and Stacey, M.G. (1998) Cloning vectors for the expression of green fluorescent protein fusion proteins in transgenic plants. *Gene*, **221**, 35–43.
- Azumi, Y., Liu, D.H., Zhao, D.Z., Li, W.X., Wang, G.F., Hu, Y. and Ma, H. (2002) Homolog interaction during meiotic prophase I in *Arabidopsis* requires the SOLO DANCERS gene encoding a novel cyclin-like protein. *EMBO J.* **21**, 3081–3095.
- Bai, X., Peirson, B.N., Dong, F., Xue, C. and Makaroff, C.A. (1999) Isolation and characterization of SYN1, a RAD21-like gene essential for meiosis in *Arabidopsis*. *Plant Cell*, **11**, 417–430.
- Baudat, F., Manova, K., Yuen, J.P., Jasin, M. and Keeney, S. (2000) Chromosome synapsis defects and sexually dimorphic meiotic progression in mice lacking Spo11. *Mol. Cell*, **6**, 989–998.
- Bhatt, A.M., Lister, C., Page, T., Franz, P., Findlay, K., Jones, G.H., Dickinson, H.G. and Dean, C. (1999) The DIF1 gene of *Arabidopsis* is required for meiotic chromosome segregation and belongs to the REC8/RAD21 cohesin gene family. *Plant J.* **19**, 463–472.
- Bishop, D.K., Park, D., Xu, L. and Kleckner, N. (1992) DMC1: a meiosis-specific yeast homolog of *E. coli* recA required for recombination, synaptonemal complex formation, and cell cycle progression. *Cell*, **69**, 439–456.
- Boisnard-Lorig, C., Colon-Carmona, A., Bauch, M., Hodge, S., Doerner, P., Bancharrel, E., Dumas, C., Haseloff, J. and Berger, F. (2001) Dynamic analyses of the expression of the HISTONE::YFP fusion protein in *Arabidopsis* show that syncytial endosperm is divided in mitotic domains. *Plant Cell*, **13**, 495–509.
- Bowman, J.L., Smyth, D.R. and Meyerowitz, E.M. (1989) Genes directing flower development in *Arabidopsis*. *Plant Cell*, **1**, 37–52.
- Buonomo, S.B., Clyne, R.K., Fuchs, J., Loidl, J., Uhlmann, F. and Nasmyth, K. (2000) Disjunction of homologous chromosomes in meiosis I depends on proteolytic cleavage of the meiotic cohesin Rec8 by separin. *Cell*, **103**, 387–398.
- Caryl, A.P., Armstrong, S.J., Jones, G.H. and Franklin, F.C.H. (2000) A homologue of the yeast HOP1 gene is inactivated in the *Arabidopsis* meiotic mutant *asy1*. *Chromosoma*, **109**, 62–71.
- Clough, S.J. and Bent, A.F. (1998) Floral dip: a simplified method for *Agrobacterium*-mediated transformation of *Arabidopsis thaliana*. *Plant J.* **16**, 735–743.
- Copenhaver, G.P., Housworth, E.A. and Stahl, F.W. (2002) Cross-over interference in *Arabidopsis*. *Genetics*, **160**, 1631–1639.
- Couteau, F., Belzile, F., Horlow, C., Grandjean, O., Vezon, D. and Doutriaux, M.P. (1999) Random chromosome segregation without meiotic arrest in both male and female meiocytes of a *dmc1* mutant of *Arabidopsis*. *Plant Cell*, **11**, 1623–1634.
- Dernburg, A.F., McDonald, K., Moulder, G., Barstead, R., Dresser, M. and Villeneuve, A.M. (1998) Meiotic recombination in *C. elegans* initiates by a conserved mechanism and is dispensable for homologous chromosome synapsis. *Cell*, **94**, 387–398.
- Fu, H., Reis, N., Lee, Y., Glickman, M.H. and Vierstra, R.D. (2001) Subunit interaction maps for the regulatory particle of the 26S proteasome and the COP9 signalosome. *EMBO J.* **20**, 7096–7107.
- Glover, J., Grelon, M., Craig, S., Chaudhury, A. and Dennis, E. (1998) Cloning and characterization of MS5 from *Arabidopsis*: a gene critical in male meiosis. *Plant J.* **15**, 345–356.
- Grelon, M., Vezon, D., Gendrot, G. and Pelletier, G. (2001) AtSPO11-1 is necessary for efficient meiotic recombination in plants. *EMBO J.* **20**, 589–600.
- Hajdukiewicz, P., Svab, Z. and Maliga, P. (1994) The small, versatile PpZp family of *Agrobacterium* binary vectors for plant transformation. *Plant Mol. Biol.* **25**, 989–994.
- Haseloff, J. (1999) GFP variants for multispectral imaging of living cells. *Meth. Cell Biol.* **58**, 139–151.
- Hollingsworth, N.M., Goetsch, L. and Byers, B. (1990) The *Hop1* gene encodes a meiosis-specific component of yeast chromosomes. *Cell*, **61**, 73–84.
- Ijichi, H., Tanaka, T., Nakamura, T., Yagi, H., Hakuba, A. and Sato, M. (2000) Molecular cloning and characterization of a human homologue of TBPIP, a BRCA1 locus-related gene. *Gene*, **248**, 99–107.
- Jefferson, R.A. (1988) Plant reporter genes: the GUS gene fusion system. In *Genetic Engineering* (Setlow, J.K., ed.). Vol. 10. New York: Plenum Publishers Co., pp. 247–263.
- Keeney, S. (2001) Mechanism and control of meiotic recombination initiation. *Curr. Topic Dev. Biol.* **52**, 1–53.
- Klapholz, S., Waddell, C.S. and Esposito, R.E. (1985) The role of the SPO11 gene in meiotic recombination in yeast. *Genetics*, **110**, 187–216.
- Klein, F., Mahr, P., Galova, M., Buonomo, S.B., Michaelis, C., Nairz, K. and Nasmyth, K. (1999) A central role for cohesins in sister chromatid cohesion, formation of axial elements, and recombination during yeast meiosis. *Cell*, **98**, 91–103.
- Ko, L., Cardona, G.R., Henrion-Caude, A. and Chin, W.W. (2002) Identification and characterization of a tissue-specific coactivator, GT198, that interacts with the DNA-binding domains of nuclear receptors. *Mol. Cell Biol.* **22**, 357–369.
- Krizek, B.A. and Meyerowitz, E.M. (1996) The *Arabidopsis* homeotic genes APETALA3 and PISTILLATA are sufficient to provide the B class organ identity function. *Development*, **122**, 11–22.
- Lee, B. and Amon, A. (2001) Meiosis: how to create a specialized cell cycle. *Curr. Opin. Cell Biol.* **13**, 770–777.
- Leu, J.Y., Chua, P.R. and Roeder, G.S. (1998) The meiosis-specific Hop2 protein of *S. cerevisiae* ensures synapsis between homologous chromosomes. *Cell*, **94**, 375–386.
- Liu, Y.G. and Whittier, R.F. (1995) Thermal asymmetric interlaced PCR – automatable amplification and sequencing of insert end fragments from P1 and Yac clones for chromosome walking. *Genomics*, **25**, 674–681.
- Loidl, J., Klein, F. and Scherthan, H. (1994) Homologous pairing is reduced but not abolished in asynaptic mutants of yeast. *J. Cell Biol.* **125**, 1191–1200.
- McKim, K.S. and Hayashi-Hagihara, A. (1998) mei-W68 in *Drosophila melanogaster* encodes a Spo11 homolog: evidence that the mechanism for initiating meiotic recombination is conserved. *Genes Dev.* **12**, 2932–2942.
- Mercier, R., Vezon, D., Bullier, E., Motamayor, J.C., Sellier, A., Lefevre, F., Pelletier, G. and Horlow, C. (2001) SWITCH1 (SWI1): a novel protein required for the establishment of sister chromatid cohesion and for bivalent formation at meiosis. *Genes Dev.* **15**, 1859–1871.
- Moffatt, B.A., McWhinnie, E.A., Agarwal, S.K. and Schaff, D.A. (1994) The adenine phosphoribosyltransferase-encoding gene of *Arabidopsis thaliana*. *Gene*, **143**, 211–216.
- Nabeshima, K., Kakahara, Y., Hiraoka, Y. and Nojima, H. (2001) A novel meiosis-specific protein of fission yeast, Meu13p, promotes homologous pairing independently of homologous recombination. *EMBO J.* **20**, 3871–3881.
- Pasierbek, P., Jantsch, M., Melcher, M., Schleiffer, A., Schweizer, D. and Loidl, J. (2001) A *Caenorhabditis elegans* cohesion

- protein with functions in meiotic chromosome pairing and disjunction. *Genes Dev.* **15**, 1349–1360.
- Roeder, G.S.** (1997) Meiotic chromosomes: it takes two to tango. *Genes Dev.* **11**, 2600–2621.
- Roeder, G.S. and Bailis, J.M.** (2000) The pachytene checkpoint. *Trends Genet.* **16**, 395–403.
- Romanienko, P.J. and Camerini-Otero, R.D.** (2000) The mouse Spo11 gene is required for meiotic chromosome synapsis. *Mol. Cell.* **6**, 975–987.
- Sambrook, J., Fritsch, E.F. and Maniatis, T.** (1989) *Molecular Cloning – a Laboratory Manual*, 2nd edn. Cold Spring Harbor: Cold Spring Harbor Laboratory Press.
- Schwarzmaier, T. and Heslop-Harrison, P.** (2000) *Practical In Situ Hybridisation*. New York: Springer-Verlag New York Inc./BIOS Scientific Publishers Ltd.
- Shinohara, A., Ogawa, H. and Ogawa, T.** (1992) Rad51 protein involved in repair and recombination in *S. cerevisiae* is a RecA-like protein. *Cell*, **69**, 457–470.
- Sym, M., Engebrecht, J.A. and Roeder, G.S.** (1993) ZIP1 is a synaptonemal complex protein required for meiotic chromosome synapsis. *Cell*, **72**, 365–378.
- Tanaka, T., Nakamura, T., Takagi, H. and Sato, M.** (1997) Molecular cloning and characterization of a novel TBP-1 interacting protein (TBPIP): enhancement of TBP-1 action on Tat by TBPIP. *Biochem. Biophys. Res. Commun.* **239**, 176–181.
- Tsubouchi, H. and Roeder, G.S.** (2002) The Mnd1 protein forms a complex with hop2 to promote homologous chromosome pairing and meiotic double-strand break repair. *Mol. Cell Biol.* **22**, 3078–3088.
- Valvekens, D., Vanmontagu, M. and Vanlijsebettens, M.** (1988) *Agrobacterium tumefaciens*-mediated transformation of *Arabidopsis thaliana* root explants by using kanamycin selection. *Proc. Natl. Acad. Sci. USA*, **85**, 5536–5540.
- Varagona, M.J., Schmidt, R.J. and Raikhel, N.V.** (1992) Nuclear localization signal(s) required for nuclear targeting of the maize regulatory protein Opaque-2. *Plant Cell*, **4**, 1213–1227.
- Villeneuve, A.M. and Hillers, K.J.** (2001) Whence meiosis? *Cell*, **106**, 647–650.
- Watanabe, Y. and Nurse, P.** (1999) Cohesin Rec8 is required for reductional chromosome segregation at meiosis. *Nature*, **400**, 461–464.
- Weiner, B.M. and Kleckner, N.** (1994) Chromosome pairing via multiple interstitial interactions before and during meiosis in yeast. *Cell*, **77**, 977–991.
- Zetka, M.C., Kawasaki, I., Strome, S. and Muller, F.** (1999) Synapsis and chiasma formation in *Caenorhabditis elegans* require HIM-3, a meiotic chromosome core component that functions in chromosome segregation. *Genes Dev.* **13**, 2258–2270.
- Zickler, D. and Kleckner, N.** (1999) Meiotic chromosomes: integrative structure and function. *Annu. Rev. Genet.* **33**, 603–754.

The GenBank accession number for the AHP2 cDNA is AY225519.